

## Video Article

# PET and MRI Guided Irradiation of a Glioblastoma Rat Model Using a Micro-irradiator

Julie Bolcaen<sup>1</sup>, Benedicte Descamps<sup>2</sup>, Tom Boterberg<sup>3</sup>, Christian Vanhove<sup>2</sup>, Ingeborg Goethals<sup>1</sup><sup>1</sup>Department of Nuclear Medicine, Ghent University Hospital<sup>2</sup>IBiTech-MEDISIP, Department of Electronics and Information Systems, Ghent University<sup>3</sup>Department of Radiation Oncology, Ghent University HospitalCorrespondence to: Julie Bolcaen at [julie.bolcaen@ugent.be](mailto:julie.bolcaen@ugent.be)URL: <https://www.jove.com/video/56601>DOI: [doi:10.3791/56601](https://doi.org/10.3791/56601)

Keywords: Cancer Research, Small animal irradiation, glioblastoma, magnetic resonance imaging, positron emission tomography, image-guided irradiation

Date Published: 12/9/2017

Citation: Bolcaen, J., Descamps, B., Boterberg, T., Vanhove, C., Goethals, I. PET and MRI Guided Irradiation of a Glioblastoma Rat Model Using a Micro-irradiator. *J. Vis. Exp.* (), e56601, doi:10.3791/56601 (2017).

## Abstract

For decades, small animal radiation research was mostly performed using fairly crude experimental setups applying simple single-beam techniques without the ability to target a specific or well-delineated tumor volume. The delivery of radiation was achieved using fixed radiation sources or linear accelerators producing megavoltage (MV) X-rays. These devices are unable to achieve sub-millimeter precision required for small animals. Furthermore, the high doses delivered to healthy surrounding tissue hamper response assessment. To increase the translation between small animal studies and humans, our goal was to mimic the treatment of human glioblastoma in a rat model. To enable a more accurate irradiation in a preclinical setting, recently, precision image-guided small animal radiation research platforms were developed. Similar to human planning systems, treatment planning on these micro-irradiators is based on computed tomography (CT). However, low soft-tissue contrast on CT makes it very challenging to localize targets in certain tissues, such as the brain. Therefore, incorporating magnetic resonance imaging (MRI), which has excellent soft-tissue contrast compared to CT, would enable a more precise delineation of the target for irradiation. In the last decade also biological imaging techniques, such as positron emission tomography (PET) gained interest for radiation therapy treatment guidance. PET enables the visualization of e.g., glucose consumption, amino-acid transport, or hypoxia, present in the tumor. Targeting those highly proliferative or radio-resistant parts of the tumor with a higher dose could give a survival benefit. This hypothesis led to the introduction of the biological tumor volume (BTV), besides the conventional gross target volume (GTV), clinical target volume (CTV), and planned target volume (PTV).

At the preclinical imaging lab of Ghent University, a micro-irradiator, a small animal PET, and a 7 T small animal MRI are available. The goal was to incorporate MRI-guided irradiation and PET-guided sub-volume boosting in a glioblastoma rat model.

## Video Link

The video component of this article can be found at <https://www.jove.com/video/56601/>

## Introduction

High-grade glioma is the most common and most aggressive malignant brain tumor in adults with a median survival of 1 year despite current treatment modalities. The standard of care includes maximal surgical resection followed by combined external beam radiation therapy (RT) and temozolomide (TMZ), followed by maintenance TMZ<sup>1,2,3</sup>. Since the introduction of TMZ now more than 15 years ago, no significant improvements have been made in the treatment of these tumors. Therefore, the implementation of new therapeutic strategies is urgent but should be first investigated in small animal cancer therapy models (mostly mice and rats). Tumor-bearing rodent models can be used to investigate the efficacy of new and complex radiation protocols, possibly combined with other (new) treatment agents, to assess radiation response or to investigate radio-protective agents. A major advantage of preclinical radiation research is the ability to work under controlled experimental conditions using large cohorts resulting in accelerated data yield due to the shorter lifespans of rodents. The preclinical findings should then be translated into a clinical trial in a much faster and more efficient way than in current practice<sup>4</sup>.

Small animal radiation experiments in the last decades have typically been achieved using fixed radiation sources<sup>5,6,7</sup> e.g., <sup>137</sup>Cs and <sup>60</sup>Co, isotopes, or linear accelerators intended for human clinical use, applying a single radiation field with MV X-rays<sup>6,8,9,10,11</sup>. However, these devices do not reach sub-millimeter precision, which is required for small animals<sup>12</sup>. Furthermore, MV X-rays have characteristics unsuitable for irradiating small targets, such as a dose build-up at the air-tissue interface in the entrance region of the beam with an extent in the order of the animal size itself<sup>4,6,8,9,10,11</sup>. The latter makes it quite challenging to deliver a uniform dose to a tumor while sparing surrounding normal brain tissue<sup>4,8,9,10,11</sup>. Hence, it is unclear to which extent current animal studies still are relevant for modern RT practice<sup>12</sup>. In this respect, recently developed three-dimensional (3D) conformal small animal micro-irradiators are promising to bridge the technological gap between advanced 3D image-guided RT techniques, such as intensity modulated radiation therapy (IMRT) or conformal arcs used in humans and current small animal irradiation<sup>4,13</sup>. These platforms make use of a kilovoltage (kV) X-ray source to obtain sharp penumbras and to avoid dose build-up. These

platforms include a computer-controlled stage for animal positioning, a kV X-ray source for imaging and radiation treatment, a rotational gantry assembly to allow radiation delivery from various angles, and a collimating system to shape the radiation beam<sup>4</sup>. In 2011, a micro-irradiator was installed at the preclinical imaging lab of Ghent University (**Figure 1**). This system is similar to modern human radiotherapy practice and enables a wide variety of preclinical experiments, such as the synergy of radiation with other therapies, complex radiation schemes, and image-guided sub-target boost studies.

Treatment planning on these micro-irradiators is based on CT, which is equivalent to human planning systems<sup>14,15</sup>. For CT imaging, an on-board X-ray detector is used in combination with the same kV X-ray tube that is used during treatment. CT imaging is used as it allows for accurate animal positioning and provides information necessary for individual radiation dose calculations via segmentation. However, due to the low soft-tissue contrast in CT imaging, tumors in the brain of small animals, such as high-grade glioma, cannot be easily delineated. The incorporation of multi-modality imaging is therefore necessary for an accurate target volume delineation. Compared to CT, MRI provides vastly superior soft-tissue contrast. This makes it much easier to visualize lesion boundaries that will result in a much better delineation of the target volume, helping to better irradiate the lesion and avoid surrounding tissue, as illustrated in **Figure 2**<sup>4,16</sup>. An additional advantage is that MRI uses non-ionizing radiation, unlike CT that is using ionizing radiation. The major disadvantages of MRI are the relatively long acquisition times and high operational costs. It is important to note that MRI scans cannot be used for dose calculations, as they do not provide the required electron density information, although progress is being made in this field, too with the recent development of MR-LINACS. As such, a combined CT/MRI dataset is the method of choice for planning the irradiation of malignant glioma, containing both the information required for targeting (MRI-based volumes) and for dose calculations (CT-based electron density).

To decrease the gap between small animal irradiation and clinical routine, MRI clearly needs to be integrated into the work flow of the micro-irradiator, requiring a correct registration between MRI and CT, which is far from trivial. In this paper, our protocol for MRI-guided 3D conformal irradiation of F98 glioblastoma in rats is discussed, which has been published recently<sup>17</sup>.

Although incorporating CT and MRI in the workflow of the micro-irradiator is a clear step forward in small animal irradiation research, these anatomical imaging techniques do not always allow a full definition of the target volume. Pathological changes in the brain on CT and MRI are characterized by increased water content (edema) and leakage of the blood-brain barrier or contrast enhancement. However, both contrast-enhancement and hyper-intense areas on T2-weighted MRI are not always an accurate measure of tumor extent. Tumor cells have been detected far beyond the margins of contrast-enhancement<sup>12</sup>. Also, none of these techniques can identify the most aggressive parts within the tumor, which may be responsible for therapeutic resistance and tumor recurrence. Therefore, additional information from molecular imaging techniques like PET may have an added value for RT target volume definition because these techniques enable to visualize biologic pathways *in vivo*<sup>12,18,19</sup>.

In 2000, Ling *et al.* introduced the concept of biological target volume (BTV) by integrating anatomical and functional imaging into the radiotherapy workflow, leading to what they called multidimensional conformal radiotherapy<sup>20</sup>. This creates the possibility to improve dose targeting by delivering a non-uniform dose to a target region using for example PET images. The most widely used PET tracer for tumor staging and to monitor treatment response is fluor-18 (<sup>18</sup>F) labeled fluorodeoxyglucose (FDG), which visualizes the glucose metabolism<sup>21</sup>. In head and neck cancer, previous studies have shown that the use of <sup>18</sup>F-FDG PET led to a better estimate of the actual tumor volume, as defined by the pathologic specimens, compared with CT and MRI<sup>22</sup>. In primary brain tumors, where FDG is not useful due to the very strong background signal from the normal brain, amino acids, such as <sup>11</sup>C-methionine and more recently <sup>18</sup>F-fluoroethyltyrosine (FET), have been investigated for GTV delineation with often marked differences between amino-acid PET and MRI-based GTVs<sup>23</sup>. However, no prospective trial investigating the meaning of this finding has been performed yet. In this study, we selected the amino-acid tracer <sup>18</sup>F-FET and the hypoxia tracer <sup>18</sup>F-fluoroazomycin-arabinozide (<sup>18</sup>F-FAZA). <sup>18</sup>F-FET and <sup>18</sup>F-FAZA were selected because an increased amino-acid uptake is strongly correlated with the proliferation rate in GB tumors, whereas uptake of a hypoxia PET-tracer is correlated with resistance to (chemo)radiotherapy<sup>18,23</sup>. Sub-volume boosting using the micro-irradiator was optimized by giving an additional radiation dose to a PET-defined part of the F98 GB tumor in rats.

## Protocol

The study was approved by the ethics committee for animal experiments (ECD 09/23 and ECD 12/28). All commercial details can be found in **Table of Materials**.

### 1. F98 GB Rat Cell Model

1. Culture the F98 GB cells, obtained from ATCC, in monolayers using Dulbecco's modified Eagle Medium, 10% calf serum, 1% penicillin, 1% streptomycin, 1% L-glutamine, and 0.1% amphotericin b, and place in a CO<sub>2</sub> incubator (5% CO<sub>2</sub> and 37 °C).
2. Inoculate the glioma cells in the brain of female Fischer F344 rats (body weight 170 g).
  1. Use sterile instruments and wear sterile gloves at all times.
  2. Anesthetize the rats by injecting a mixture of 74 mg/kg ketamine and 11 mg/kg xylazine intraperitoneally (IP) with an insulin syringe (1 mL, 29 G). Confirm the anesthetization by the absence of response to the withdrawal reflex of the limb. Immobilize the rats in a stereotactic device using fixation points for nose and ears. Place a carbomer eye gel to prevent dryness of the eyes while under anesthesia.
  3. Shave the rat from eye level to the back of the skull and disinfect the skin with povidone-iodine.
  4. Expose the skull through a midline scalp incision of 2 cm, and make a 1 mm hole (diamond drill) 2 mm posterior and 2.5 mm lateral to the bregma in the right frontal hemisphere.
  5. Insert a stereotactically guided insulin needle (29 G) and inject 5 µL cell suspension (20,000 F98 GB cells) 3 mm deep using an microsyringe pump controller (settings: inject (I50), rate 1 nL/s (001 SDN)).
  6. Withdraw the syringe slowly and close the incision with bone wax. Suture the skin and disinfect with povidone-iodine.
  7. Stabilize the body temperature of the animal post-surgery using a red lamp. Monitor the awakening of the rat until it has regained sufficient consciousness to maintain sternal recumbency. Do not return the animal to the company of other animals until fully recovered.

Keep all animals under environmentally controlled conditions (12 h normal light/dark cycles, 20-24 °C, and 40-70% relative humidity) with food and water *ad libitum*. Make sure to follow the animals closely by monitoring their body weight, food, water intake, and their activity and normal behavior. Use a lethal dose of pentobarbital sodium to euthanize the animals (160 mg/kg) if a decline of 20% body weight is observed or when the normal behavior severely deteriorates (e.g., lack of grooming).

## 2. Confirmation of Tumor Growth

NOTE: Evaluate tumor growth 8 days post-inoculation using T2-weighted MRI, dynamic contrast-enhanced MRI (DCE-MRI), and contrast-enhanced T1-weighted MRI. When the tumor reaches a size of 2.5 x 2.5 x 2.5 mm<sup>3</sup>, select the rat for therapy.

1. First, connect a 30 G needle to a 60 cm long tube, which is placed intravenously in the lateral tail vein. Anesthetize the rats through a nose cone with 2% isoflurane mixed with oxygen (0.3 L/min). Confirm anesthetization when the rats do not respond to the withdrawal reflex of the limb. Cover the rats with a heated blanket and place them in the MRI bed. Use a carbomer eye gel to prevent dryness.
2. Place the bed in the holder with a fixed rat brain surface coil, and position the bed in a 72 mm rat whole body transmitter coil.
3. Perform a localizer scan followed by a T2-weighted spin-echo scan to assess tumor growth. T2-MRI sequence details: TR/TE 3661/37.1 ms, 109 μm isotropic in-plane resolution, slice thickness 600 μm, 4 averages, TA 9 min 45 s.
4. If tumor is confirmed on the T2-weighted acquisition, inject a gadolinium-containing contrast agent into the intravenously placed tubing (MRI contrast agent; 0.4 mL/kg) 30 s after the start of the DCE-MRI acquisition. Acquire DCE-MRI during 12 min using a fast-low angle shot (FLASH) sequence in a single slice (1 mm slice thickness). Use an in-plane spatial resolution of (312 μm<sup>2</sup>) and a temporal resolution of 1.34 s.
5. Using the image sequence analysis tool, select a region of interest (ROI) within the suspected tumor region to plot the signal intensity over time. Subsequently, analyze the shape of the resulting DCE curve to confirm the presence of glioblastoma (**Figure 3**).
6. Finally, acquire a contrast-enhanced T1-weighted spin-echo sequence. T1-MRI sequence details: TR/TE 1539/9.7 ms, 117 μm isotropic in-plane resolution, slice thickness 600 μm, 3 averages, TA 4 min 15 s. Typical contrast-enhanced T1-weighted MR images are shown in **Figure 2**.
7. After finalizing the T1-weighted sequence, the animal can wake up under continuous supervision, until it regains full consciousness.

## 3. Multimodality Imaging for Target Volume Selection

NOTE: To be able to perform MRI-guided 3D conformal irradiation of the F98 GB rat model with PET-guided sub-volume boosting, 3 imaging modalities need to be performed. First, inject the radiotracer, then perform MRI during tracer uptake, subsequently perform a static PET acquisition and a treatment planning CT.

1. Anesthetize the animals using a nose cone with 2% isoflurane mixed with oxygen (0.3 L/min). Confirm anesthetization when the rats do not respond to the withdrawal reflex of the limb. Use a carbomer eye gel to prevent dryness while under anesthesia.
2. Insert a catheter (26 G) into the tail vein, enabling the injection of 37 MBq of PET radioactive tracer dissolved in 200 μL saline. Inject either <sup>18</sup>F-FET or <sup>18</sup>F-FAZA, 30 min or 2 h before PET acquisition, respectively.
3. Inject MRI contrast agent (0.4 mL/kg) intravenously in the tail vein using the catheter 15 min before PET acquisition.
4. Place the rats on an in-house made multimodality bed and secure using hook-and-loop fasteners, maintaining a fixed position during imaging and micro-irradiation (**Figure 1**).
5. Fix three multimodality markers (capillaries filled with water) underneath, above, and on the right side of the skull. Place the rat, still fixed on the multimodality bed, in the animal holder of the MRI scanner, fix the rat brain surface coil and position this set-up in a 72 mm rat whole-body transmitter coil. Perform a localizer scan followed by a contrast-enhanced T1-weighted spin-echo sequence.
6. Transport the animal to perform a <sup>18</sup>F-FET or <sup>18</sup>F-FAZA PET acquisition. Acquire a 30 min static PET scan in list-mode. Scan should be acquired either 30 min after <sup>18</sup>F-FET injection or 2 h after <sup>18</sup>F-FAZA injection. Reconstruct all PET scans into a 200 × 200 × 64 matrix by a 2D Maximum Likelihood Expectation Maximization (MLEM) algorithm using 60 iterations and a voxel size of 0.5 × 0.5 × 1.157 mm.
7. Place the animal, still fixed on the multimodality bed, on a plastic holder secured onto the four-axis robotic positioning table of the micro-irradiator. Perform a high-resolution treatment planning CT scan using an aluminum filter of 1 mm and a 20 × 20 cm (1,024 × 1,024 pixel) amorphous Si flat panel detector. Reconstruct the CT images with an isotropic voxel size of 0.2 mm. Fix the tube voltage and tube current at 70 kV and 0.4 mA, respectively. Acquire a total of 360 projections over 360 °.

## 4. RT Treatment Planning

1. Use the pre-clinical treatment planning system (PCTPS) for treatment planning. Import the planning CT into the PCTPS and manually segment this CT image into three different tissue classes: bone, soft tissue, and air. This manual segmentation is based on defining three different grey-value thresholds on the planning CT. These manually selected grey-value thresholds should be chosen such that air in the brain is absent and that bone thickness of the skull is non-zero. Once these thresholds are defined, material densities are assigned by the PCTPS for bone, soft tissue, and air (**Figure 4**).
2. If only MRI guidance is needed, load the MRI scan and co-register with the planning CT using the PCTPS.
  1. Use rigid body transformations (three translations and three rotations), the multimodality markers, and the skull. By overlaying the increased signal intensity of the skull on CT with black signal on MRI, a precise fusion can be achieved (**Figure 5**).
  2. Select the target for irradiation in the center of the contrast-enhancing tumor on T1-weighted MRI, see **Figure 6** and **Figure 7**.
3. When additional PET information must be included, include a CT/MRI/PET co-registration using the biomedical image quantification software (BIQS).

1. Use the contouring tool in the BIQS to achieve PET/MRI image fusion (**Figure 8**). After co-registration, select the target in the center of the increased PET tracer uptake in the BIQS (**Figure 9**) and enter the coordinates manually into the PCTPS using the following transformations:  $X \rightarrow -X$ ,  $Y \rightarrow Z$ , and  $Z \rightarrow -Y$ .
  2. Select the prescribed dose, number of arcs, arc position, rotation range of the arcs, and the collimator size (**Figure 10**).
  3. For MRI-guided RT, use the following settings: a prescribed dose of 20 Gy, 3 arcs positioned at couch angles of  $-45^\circ$ ,  $0^\circ$ , and  $45^\circ$  with arc rotations of  $120^\circ$ , and a collimator size of 5 x 5 mm.
  4. For PET-MRI-guided RT, use the following settings: a prescribed dose of 20 Gy using 3 arcs and a 5 x 5 mm collimator and extra 5 Gy for sub-volume boosting using 3 non-coplanar arcs and a 1 x 1 mm collimator. Select a rotation of  $120^\circ$  for all arcs while changing the position of the couch ( $-45^\circ$ ,  $0^\circ$ , and  $45^\circ$ ).
4. Calculate the dose distribution within the animal and the beam delivery parameters to deliver the prescribed dose to the target using the PCTPS. Before actual irradiation, test the arc rotations at the different couch positions to prevent any collision during irradiation.
  5. For the actual irradiation, select a 0.15 mm copper filter, set the X-ray voltage to 220 kV, set the X-ray current to 13 mA, and position the right collimator on the gantry. Execute the RT by transferring the appropriate beam delivery parameters from the PCTPS to the micro-irradiator.
  6. During these procedures, the rat is kept under continuous isoflurane anesthesia (2% isoflurane, mixed with oxygen 0.3 L/min). Following the execution of the last arc, the animal can wake up under continuous supervision, until it regains full consciousness.

## 5. Dose Volume Histograms (DVHs)

NOTE: To compare the actual dose delivered to the tumor target volumes and the surrounding normal brain tissue, calculate DVHs.

1. Draw a volume-of-interest (VOI) around the tumor and the normal brain on the T1-weighted contrast-enhanced MR images to calculate the mean, maximum, and minimum dose (**Figure 11**).
2. As a surrogate for the maximal, mean, and minimal dose to the tumor volume and the normal brain tissue volume, calculate the  $D_2$ ,  $D_{50}$ , and  $D_{90}$ .  $D$  stands for the dose received by  $x\%$  of the volume, denoted by the subscript, and can be derived from the resulting DVH.

## 6. TMZ and Sham Chemotherapy

1. To mimic the treatment of glioblastoma in patients, administer concomitant chemotherapy using IP injections of 29 mg/kg TMZ dissolved in saline with 25% dimethylsulfoxide (DMSO) once a day for 5 days starting at the day of irradiation<sup>24,25</sup>. Use 1 mL, 29 G insulin syringe to administer injection.
2. For the control group, administer injection from step 6.1 without TMZ.

## Representative Results

To mimic the human treatment methodology for the irradiation of glioblastoma in a preclinical model, inclusion of MRI-guided radiotherapy was necessary. Using the PCTPS and the micro-irradiator interface we were able to irradiate F98 glioblastoma in rats with multiple conformal non-coplanar arcs targeting the contrast-enhanced region on T1-weighted MRI<sup>17</sup>. Rigid-body transformations in combination with a multi-modality bed were used for image registration between MRI and planning CT. The isocenter for irradiation was selected in the center of the contrast-enhanced tumor region on T1-weighted MRI (**Figure 7**).

Dose distributions and cumulative DVHs of the mean, minimal, and maximal dose of the target volume and the normal brain tissue volume were calculated for five different animals (**Figure 12**). Based on the similarity with the clinical irradiation protocol and an optimal dose distribution, a dose plan using three non-coplanar arcs was selected. Applying the latter, 90% of the target volume received the desired dose, while minimizing the dose to normal brain tissue<sup>17</sup>.

After confirming the feasibility of MRI-guided irradiation of the F98 rat glioblastoma model, we tried to incorporate PET-based sub-volume boosting in the preclinical workflow for RT planning. We were able to combine 3 imaging modalities, performing first MRI, then PET, and finally CT while the rat is fixed on an in-house made multimodality bed (**Figure 1**). For co-registration of these modalities, we used the BIQS, enabling a lot more tools for rigid matching (**Figure 8**). Applying a simple transformation, both the MR based and PET based isocenter (**Figure 9**) could be transferred to the PCTPS. In **Figure 13**, both the MRI and PET-based isocenter for irradiation after dose calculation in the PCTPS are shown. To irradiate the entire contrast-enhancing volume we selected a 5 x 5 collimator and three arcs rotating  $120^\circ$ . For boosting the most metabolically active tumor part identified on  $^{18}\text{F}$ -FET PET or the most hypoxic tumor part identified on  $^{18}\text{F}$ -FAZA PET, a dose of 5 Gy was selected and delivered using a collimator of 1 mm diameter. Again, 3 arcs rotating  $120^\circ$  are applied.

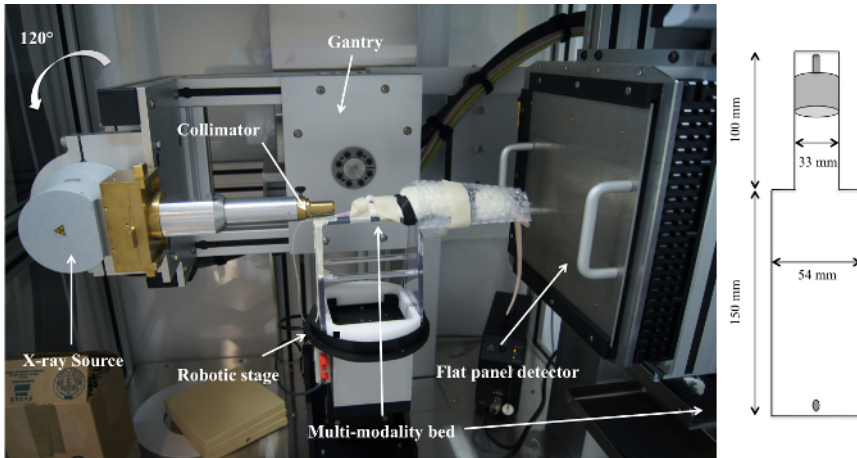


**Figure 1:** Micro-irradiator integrating a kV X-ray tube, a rotating gantry, a computer-controlled robotic stage, a collimating system to shape the beam, and a flat-panel CT detector. The animal is placed on a 4 mm thick PVC multimodality bed to prevent movements between multiple imaging acquisitions, such as an MRI scan followed by a planning CT, which facilitates image fusion. [Please click here to view a larger version of this figure.](#)

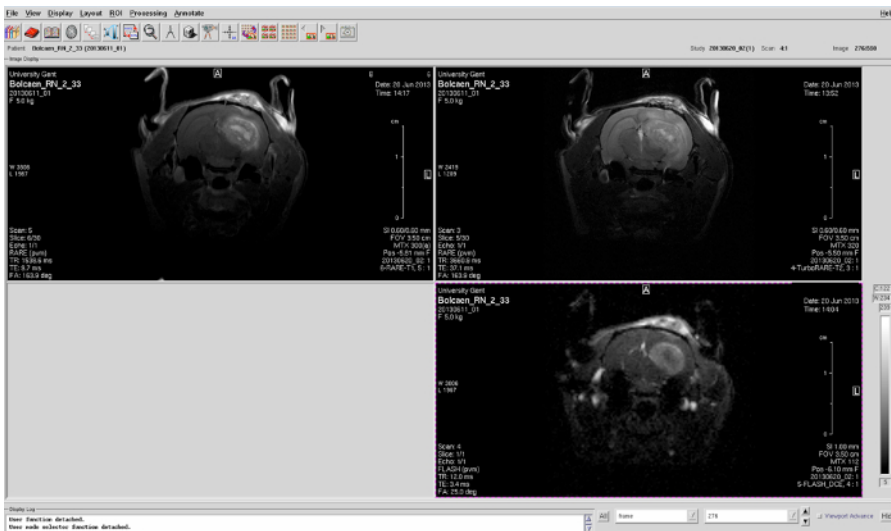


**Figure 2:** Glioblastoma confirmation. T1-weighted MRI, T2-weighted MRI, and DCE-MRI of a F98 GB rat. [Please click here to view a larger version of this figure.](#)

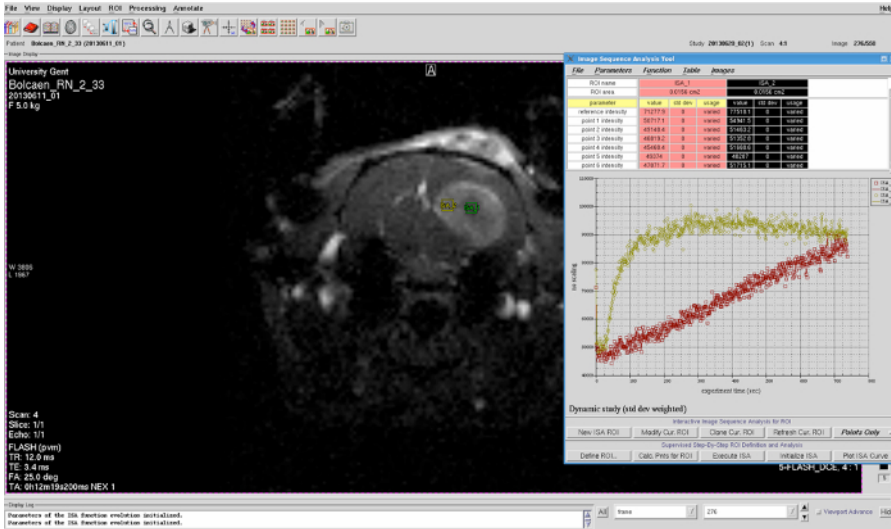


**Figure 3: DCE curve.** Using the image sequence analysis tool, a ROI can be selected on the DCE-MRI scan to plot the signal intensity over time. Subsequently, analysis of the shape of the resulting DCE curve is able to confirm the presence of glioblastoma. [Please click here to view a larger version of this figure.](#)

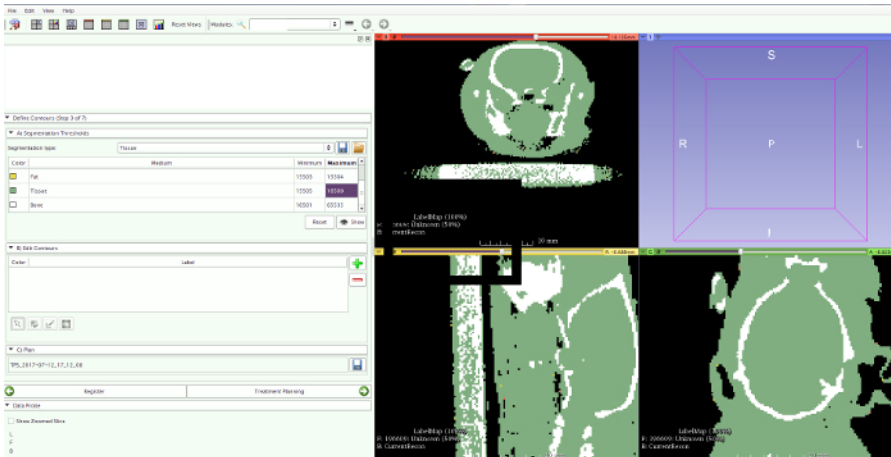


**Figure 4: CT segmentation.** Segmentation based on CT is done by manually defining a number of threshold values to accurately distinguish air from lung tissue, fat tissue, bone, and other tissues within the image. [Please click here to view a larger version of this figure.](#)

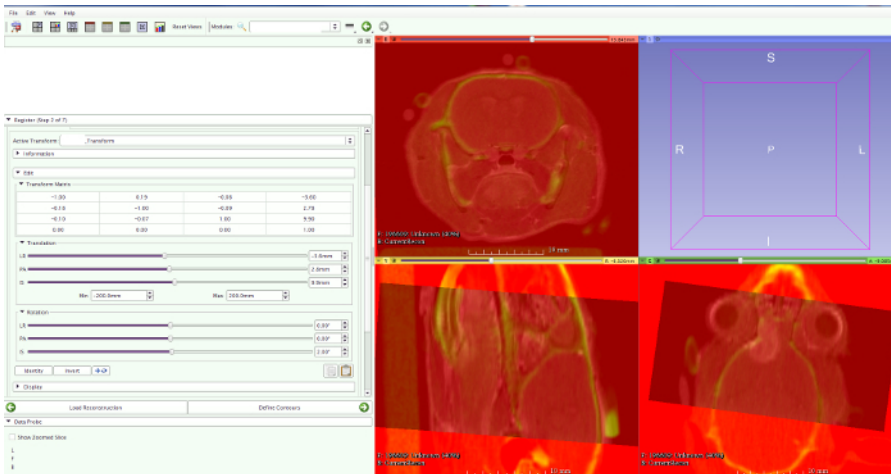


**Figure 5: MRI-CT fusion.** By overlaying the increased signal intensity of the skull on CT with black signal on MRI, a precise fusion can be achieved. [Please click here to view a larger version of this figure.](#)

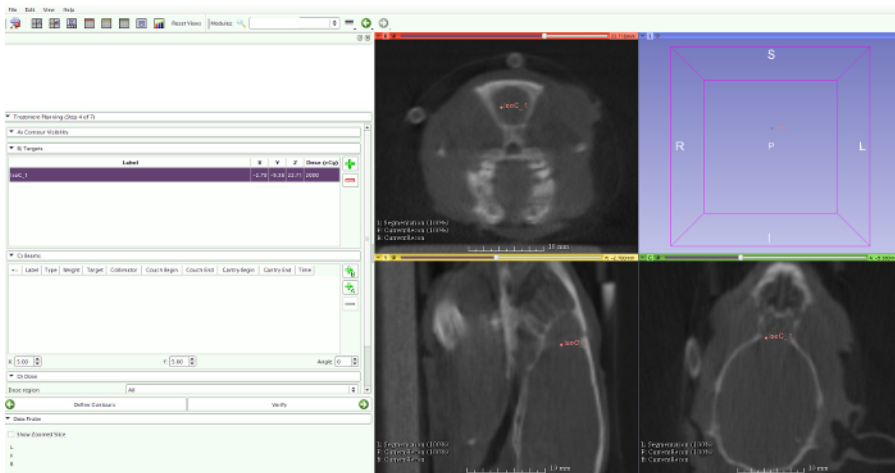


**Figure 6: Cone beam CT.** No tumor is visible on CT, making it impossible to select the isocenter in the center of the tumor. [Please click here to view a larger version of this figure.](#)

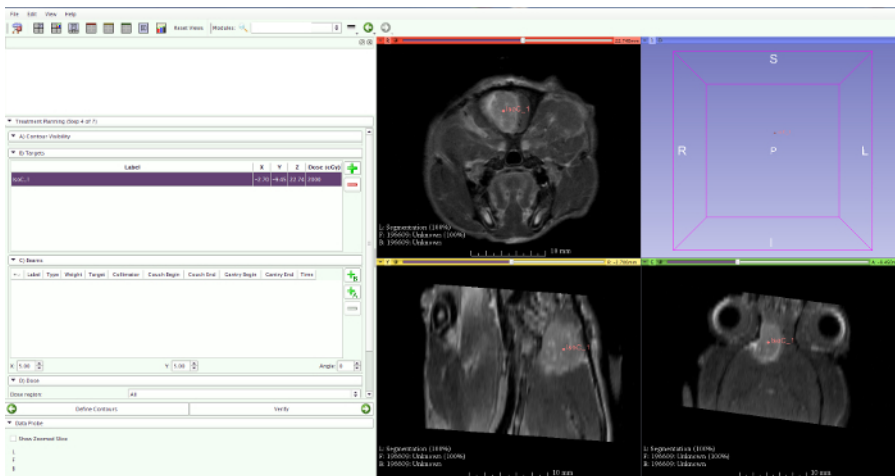


**Figure 7: Contrast-enhanced T1-weighted MRI.** The contrast-enhanced T1-weighted MRI clearly visualizes a rat F98 brain tumor. The center of the contrast-enhancement is selected as the isocenter for RT planning. [Please click here to view a larger version of this figure.](#)

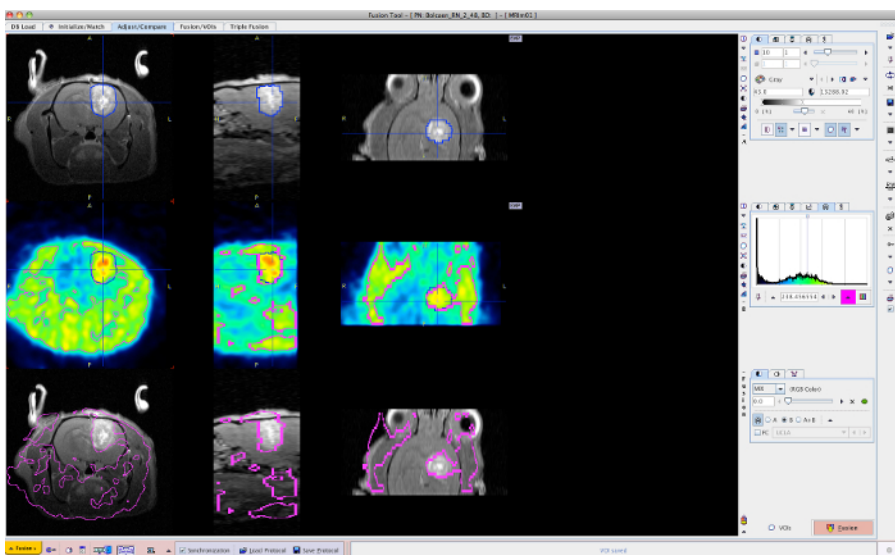


**Figure 8: MRI-PET fusion.** Using the contouring tool in the BIQS, PET/MRI image fusion is achieved. [Please click here to view a larger version of this figure.](#)

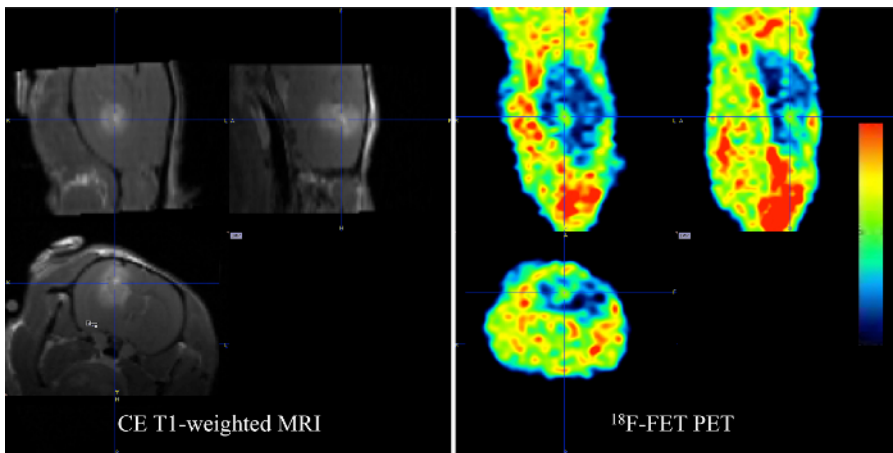


**Figure 9: MRI-PET target selection.** The target for irradiation is selected in the center of contrast-enhancement on T1-weighted MRI (left). The target for sub-volume boosting is selected in the center of the increased signal on <sup>18</sup>F-FET PET (right). [Please click here to view a larger version of this figure.](#)

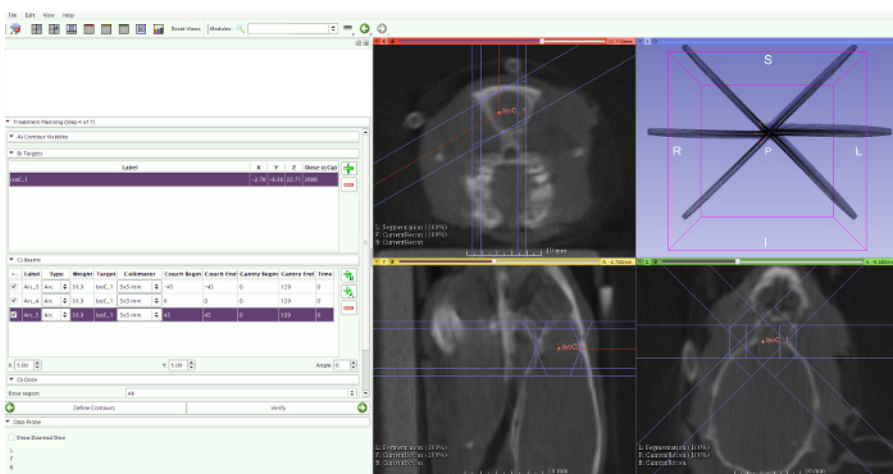


**Figure 10: Radiotherapy planning.** To calculate the radiotherapy planning, select the isocenter, prescribed dose, number of arcs, arc position, rotation range of the arcs, and the collimator size. [Please click here to view a larger version of this figure.](#)

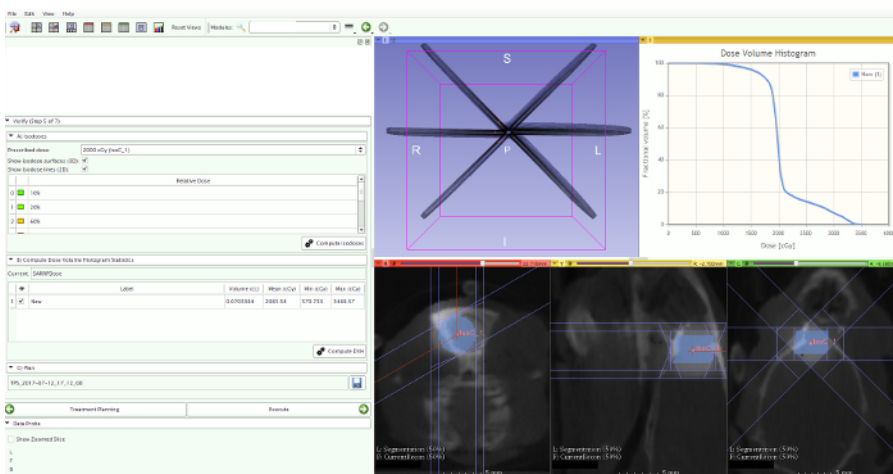


**Figure 11: DVH calculation.** Draw a volume-of-interest (VOI) around the tumor on the T1-weighted contrast-enhanced MR images to calculate the DVH within this volume. [Please click here to view a larger version of this figure.](#)



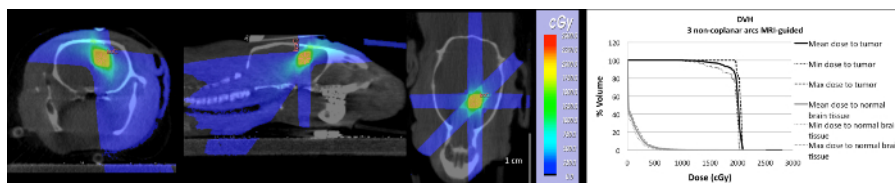


**Figure 12: Dose plan using contrast-enhanced T1-weighted MRI and three non-coplanar arcs to deliver 20 Gy to the target volume.** On the right, the cumulative Dose Volume Histogram (DVH) of the tumor volume and the normal brain tissue delineated on contrast-enhanced T1-weighted MRI is given. This figure has been modified from Bolcaen *et al.*<sup>20</sup> [Please click here to view a larger version of this figure.](#)

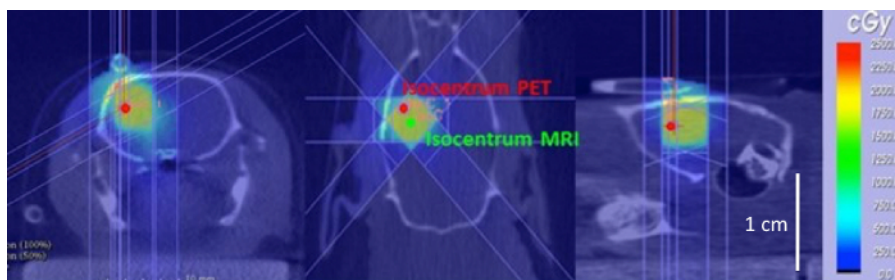


**Figure 13: Selected MRI and PET-guided isocenter for irradiation.** The CT image in axial, coronal and sagittal view is visualized with the dose plan delivering 20 Gy to the target region (yellow region). The isocenter which was identified on contrast-enhancing MRI is visible (green) and the isocenter localized on the metabolically active tumor part identified on <sup>18</sup>F-FET PET is also visible (red). [Please click here to view a larger version of this figure.](#)

## Discussion

To achieve accurate irradiation of the glioblastoma tumor target in the rat brain, the micro-irradiator's on-board CT guidance was not sufficient. Brain tumors are hardly visible due to insufficient soft tissue contrast, even if contrast enhancement would be used. As such, MRI needs to be included to allow more precise irradiation. Using a sequential MR acquisition on a 7 T system and a CT acquisition on the micro-irradiator we were able to target the dose to the contrast-enhancing tumor tissue in the brain and calculate a dose plan using the planning CT. This was feasible after image fusion and dose calculations using the PCTPS<sup>17</sup>. However, it should be kept in mind that MRI is prone to geometric distortions which are not corrected in this protocol. Moreover, before translating this irradiation protocol to other parts of the body, further research is necessary. The importance of an accurate tissue segmentation due to the use of lower kV energy photons should be considered. While segmentation into three tissue classes might be sufficient in the rat brain, more tissue classes need to be indicated in the thoracic or abdominal region of rats to provide accurate dose calculations. To avoid movement during transport between the different imaging systems, we made use of a multimodality bed which minimizes movement of the head (Figure 1). However, an additional effort is necessary when applying this protocol to other body parts, either thoracic or abdominal regions. Especially small animal irradiation of organs influenced by respiratory movement or intestinal transit is still challenging.

The incorporation of PET-guided sub-volume boosting was also shown to be feasible, despite a labor-intensive protocol. An advantage of nuclear imaging techniques, such as PET, is the ability to image the heterogeneity within tumors, which allows targeting metabolically highly active or radiation resistant parts of the tumor. We were able to increase the dose, specifically targeted on the most biologically active or most hypoxic region of the tumor using <sup>18</sup>F-FET PET or <sup>18</sup>F-FAZA PET, respectively. The critical step in the protocol is image co-registration. Currently, no software is able to automatically co-register pre-clinical MRI or CT with PET images with high enough accuracy and reproducibility. Generally, PET tracers in neuro-oncology show a low uptake in normal brain that complicates the registration process. For fusion of the three imaging modalities (CT/MRI/PET), we preferred the BIQS rather than the PCTPS, which is currently not developed to easily combine multiple imaging modalities. Furthermore, the BIQS has more smart tools for rigid matching. A major help is also the use of a multi-modality bed, preventing movement of the animal between the different imaging acquisitions. However, manual co-registration is time consuming and increases the time of anesthesia of the animals. Once image registration is achieved, exporting the coordinates from the BIQS into the PCTPS was feasible by applying a simple transformation on the target coordinates.

It is not only important to precisely target the (biological) tumor volume: sparing of the surrounding normal brain tissue has to be taken into account as well. The latter is often neglected in current animal radiotherapy experiments but very important to make the model also clinically relevant. This was achieved by applying multiple non-coplanar arcs. To our knowledge, multiple arc cranial irradiation in small animals was never applied before. With regard to beam usage, this methodology is in close resemblance with the clinical image-guided conformal RT and due to the use of arc treatment the target ultimately receives the prescribed dose, while the normal tissues only receive a fraction of it. As such, a first step is made to minimize the gap between preclinical and clinical RT technology<sup>17</sup>. A limitation of this micro-irradiator is that gantry rotation is limited to 120°. Combining arc rotations with a change in couch position further increased the sparing of normal brain tissue surrounding the tumor target.

This methodology is an important step towards inclusion of biological imaging modalities for radiotherapy guidance. However, new developments are needed to simplify pre-clinical image fusion and to incorporate dose painting by numbers (DPBN) in preclinical applications. Using the current micro-irradiator, we are now able to apply sub-volume boosting; however, DPBN is not yet possible due to limitations in dose calculations, gantry rotations, and collimator design. Finally, the development of compact preclinical PET scanners offering sub-millimeter spatial resolution is promising<sup>26</sup> and these devices might provide a very elegant solution to integrate PET into a small animal radiation platform.

We demonstrated the applicability of this model for combined MRI and PET-guided irradiation and chemotherapy of glioblastoma in rats and for future research on new therapeutics for glioblastoma. Furthermore, the application of PET-guided sub-volume boosting is a first step towards the incorporation of a BTV in the radiation treatment planning of small animal cancer models.

## Disclosures

The authors have no conflicts of interest to disclose

## Acknowledgements

The authors would like to thank Stichting Luka Hemelaere and Soroptimist International for supporting this work.

## References

1. Stupp, R., *et al.* Promising survival for patients with newly diagnosed glioblastoma multiforme treated with concomitant radiation plus temozolomide followed by adjuvant temozolomide. *J Clin Oncol.* **20** (5), 1375-1382, (2002).
2. Dhermain, F. Radiotherapy of high-grade gliomas: current standards and new concepts, innovations in imaging and radiotherapy, and new therapeutic approaches. *Chin J Cancer.* **33** (1), 16-24, (2014).
3. Ahmed, R., *et al.* Malignant gliomas: current perspectives in diagnosis, treatment, and early response assessment using advanced quantitative imaging methods. *Cancer Manag Res.* **6**, 149-170, (2014).
4. Verhaegen, F., Granton, P., Tryggstad, E. Small animal radiotherapy research platforms. *Phys Med Biol.* **56** (12), R55-R83, (2011).
5. Kinsella, T.J., Vielhuber, K.A., Kunugi, K.A., Schupp, J., Davis, T.W., Sands, H. Preclinical toxicity and efficacy study of a 14-day schedule of oral 5-iodo-2-pyrimidinone-2-deoxyribose as a prodrug for 5-iodo-2-deoxyuridine radiosensitization in U251 human glioblastoma xenografts. *Clin Cancer Res.* **6** (4), 1468-1475, (2000).
6. Vellimana, A.K., *et al.* Combination of paclitaxel thermal gel depot with temozolomide and radiotherapy significantly prolongs survival in an experimental rodent glioma model. *J Neurooncol.* **111** (3), 229-236, (2012).
7. Kioi, M., Vogel, H., Schultz, G., Hoffman, R.M., Harsh, G.R., Brown, J.M. Inhibition of vasculogenesis, but not angiogenesis, prevents the recurrence of glioblastoma after irradiation in mice. *J Clin Invest.* **120** (3), 694-705, (2010).
8. Vinchon-Petit, S., Jarnet, D., Jadaud, E., Feuvret, L., Garcion, E., Menei, P. External irradiation models for intracranial 9L glioma studies. *J Exp Clin Cancer Res.* **29**, 142, (2010).
9. Yang, W., *et al.* Convection enhanced delivery of carboplatin in combination with radiotherapy for treatment of brain tumors. *J Neurooncol.* **101** (3), 379-390, (2011).
10. Rousseau, J., *et al.* Efficacy of intracerebral delivery of cisplatin in combination with photon irradiation for treatment of brain tumors. *J Neurooncol.* **98** (3), 287-295, (2010).
11. Baumann, B.C., *et al.* An integrated method for reproducible and accurate image-guided stereotactic cranial irradiation of brain tumors using the small animal radiation research platform. *Transl Oncol.* **5** (4), 230-237, (2012).
12. Grosu, A.-L., *et al.* Implications of IMT-SPECT for postoperative radiotherapy planning in patients with gliomas. *Int J Radiat Oncol Biol Phys.* **54** (3), 842-854, (2002).
13. Butterworth, K.T., Prise, K.M., Verhaegen, F. Small animal image-guided radiotherapy: Status, considerations and potential for translational impact. *Br J Radiol.* **88** (1045), 4-6, (2015).
14. Aird, E.G.A., Conway J. CT simulation for radiotherapy treatment planning. *Br J Radiol.* **75** (900), 937-949, (2002).
15. Baker, G.R. Localization: Conventional and CT simulation. *Br J Radiol.* **79** (Spec No 1), S36-49, (2006).
16. Corroyer-Dumont, A., *et al.* MRI-guided radiotherapy of the SK-N-SH neuroblastoma xenograft model using a small animal radiation research platform. *Br J Radiol.* **90** (1069), 20160427, (2017).
17. Bolcaen, J., *et al.* MRI-guided 3D conformal arc micro-irradiation of a F98 glioblastoma rat model using the Small Animal Radiation Research Platform (SARRP). *J Neurooncol.* **120** (2), 257-266, (2014).
18. Niyazi, M., *et al.* FET-PET for malignant glioma treatment planning. *Radiother Oncol.* **99** (1), 44-48, (2011).
19. Grosu, A.L., *et al.* First experience with I-123-alpha-methyl-tyrosine SPECT in the 3-D radiation treatment planning of brain gliomas. *Int J Radiat Oncol Biol Phys.* **47** (2), 517-526, (2000).
20. Ling, C.C., *et al.* Towards multidimensional radiotherapy (MD-CRT): biological imaging and biological conformality. *Int J Radiat Oncol Biol Phys.* **47** (3), 551-560, (2000).
21. Wahl, R.L., Jacene, H., Kasamon, Y., Lodge, M.A. From RECIST to PERCIST: Evolving Considerations for PET response criteria in solid tumors. *J Nucl Med.* **50** Suppl 1 (5), 122S-150S, (2009).
22. Daisne, J.F., *et al.* Tumor volume in pharyngolaryngeal squamous cell carcinoma: comparison at CT, MR imaging, and FDG PET and validation with surgical specimen. *Radiology.* **233** (1), 93-100, (2004).
23. Grosu, A.-L., Weber, W. PET for radiation treatment planning of brain tumours. *Radiother Oncol.* Elsevier Ireland Ltd. **96** (3), 325-327, (2010).
24. Banissi, C., Ghiringhelli, F., Chen, L., Carpentier, A.F. Treg depletion with a low-dose metronomic temozolomide regimen in a rat glioma model. *Cancer Immunol Immunother.* **58**, 1627-1634, (2009).
25. Robinson, C.G., *et al.* Effect of alternative temozolomide schedules on glioblastoma O(6)-methylguanine-DNA methyltransferase activity and survival. *Br J Cancer.* **103**, 498-504, (2010).
26. España, S., Marcinkowski, R., Keereman, V., Vandenberghe, S., Van Hoken, R. DigiPET: sub-millimeter spatial resolution small-animal PET imaging using thin monolithic scintillators. *Phys Med Biol.* **59** (13), 3405, (2014).